

CONNECTION BETWEEN ACTIVE LONGITUDES AND MAGNETIC HELICITY

Axel Brandenburg¹ and Petri J. Käpylä²

¹*Nordita, Blegdamsvej 17, DK-2100 Copenhagen Ø, Denmark*

²*Kiepenheuer-Institut für Sonnenphysik, Schöneckstraße 6, D-79104 Freiburg, Germany; and
Department of Physical Sciences, Astronomy Division, P.O. Box 3000, FIN-90014 University of Oulu, Finland*

ABSTRACT

A two-dimensional mean field dynamo model is solved where magnetic helicity conservation is fully included. The model has a negative radial velocity gradient giving rise to equatorward migration of magnetic activity patterns. In addition the model develops longitudinal variability with activity patches travelling in longitude. These patches may be associated with active longitudes.

Key words: Magnetohydrodynamics (MHD) – turbulence – Sun: active longitudes.

1. INTRODUCTION

Active regions are complexes of magnetic activity out of which sunspots, flares, coronal mass ejections, and several other phenomena emerge with some preference over other regions. These regions tend to be bipolar, i.e. they come in pairs of opposite polarity and are roughly aligned with the east–west direction.

There is some controversy as to whether or not active regions appear preferentially along so-called active longitudes and what their long term stability properties are (e.g., Bai 2003, Berdyugina & Usoskin 2003, Pelt et al. 2005). Some degree of recurrence of sunspots has frequently been reported over the years (Vitinskij 1969, Bogart 1982, Bai 1987, 1988), but only now these ideas are becoming more quantitative.

As the recent analysis of Usoskin et al. (2005) has shown, active longitudes have characteristic angular velocities that depend on the phase of the cycle which, in turn, determines the typical latitude of their occurrence. The analysis of solar magnetograms by Benevolenskaya et al. (1999) showed already that at the beginning of each cycle, when most of the activity occurs at about $\pm 30^\circ$ latitude, the rotation rate of the active longitudes is $\Omega/2\pi \approx 446$ nHz, while at the end of each cycle, when the typical

latitude is only $\pm 4^\circ$ latitude, the rotation rate of the active longitudes is $\Omega/2\pi \approx 462$ nHz. The recent work of Usoskin et al. (2005) demonstrates that the active regions can also be detected in sunspot data. Unlike the analysis of Benevolenskaya et al. (1999), who isolated two different active longitudes at the beginning and the end of the cycle, Usoskin et al. (2005) determined a continuous latitudinal dependence of these active longitudes on the phase of the cycle. The success of their analysis lies in the way they calculated time-dependent reference values. In particular, they find that only 10% of the spots participate in this nonaxisymmetric effect. Thus, the effect is real, but weak, although with a well determined strength.

Given that active longitudes suggest the presence of well preserved activity patches in an otherwise turbulent medium, one has to look for a quantity that has the capability to be long-lived. An obvious candidate for anything long lived in hydromagnetic turbulence at large magnetic Reynolds numbers is the magnetic helicity. In the absence of magnetic helicity fluxes, magnetic helicity is nearly perfectly conserved in resistive magnetohydrodynamics at large magnetic Reynolds numbers. Even in the presence of magnetic helicity fluxes, magnetic helicity is only transferred from one place to another, but it is not lost. It is therefore plausible that there might be a connection between the nearly perfect magnetic helicity conservation and the long-lived features on the sun such as active longitudes. In the simplest case, magnetic helicity could be considered frozen into the plasma so that local patches of enhanced magnetic helicity would just propagate with the ambient velocity of the gas. This could in principle be a very simplistic picture of active longitudes that might explain their long life times, but not how they came into existence.

An alternative that is traditionally discussed in connection with active longitudes is the idea that there are a number of different axisymmetric and nonaxisymmetric dynamo modes present in the sun that are mixed in the right proportions such that their superposition corresponds to the observed field configuration (Rädler et al. 1990, Moss 1999, 2004, Moss & Brooke 2000, Bigazzi & Ruzmaikin 2004, Berdyugina et al. 2006). An obvious

problem is that these modes are solutions of the linearized problem and that their superposition does not constitute a solution to the nonlinear problem. At first instance only one of the modes gets selected, so the final solution is still mainly either axisymmetric or nonaxisymmetric, but not easily anything in between, as originally anticipated (Rädler et al. 1990, Moss et al. 1995).

Magnetic helicity conservation only applies to the total field, i.e. the sum of small scale and large scale fields. The large scale field produced by a mean field (large scale) dynamo does by itself not conserve magnetic helicity, because the α effect leads to a transfer of magnetic helicity from smaller to larger scales (Pouquet et al. 1976, Ji 1999). It is therefore necessary to include also the contribution from the small scale magnetic helicity, which enters into the mean field description through a magnetic contribution to the α effect. This approach is now fairly well developed and is important in reproducing the slow saturation (Field & Blackman 2002, Blackman & Brandenburg 2002, Subramanian 2002) found in simulations (Brandenburg 2001). For a review of these recent developments see Brandenburg & Subramanian (2005a).

We begin by explaining this approach in more detail. In order to focus on the essentials, we consider only a minimalistic model. The basic dynamo wave can already be described in a one-dimensional model with only latitudinal extent. In the present context we still need the longitudinal extent, but we ignore the variation of the magnetic field with depth. Furthermore, in order to study the basic effect introduced by the longitudinal extent and by magnetic helicity conservation, it suffices to restrict oneself to a cartesian model. Since there is no radial extent, there are also no radial boundaries, and hence no magnetic helicity flux out of them. This might be an important limitation to keep in mind.

2. THE MODEL

The dynamo equation together with the dynamical quenching model is (Field & Blackman 2002, Blackman & Brandenburg 2002, Subramanian 2002)

$$\frac{\partial \bar{\mathbf{B}}}{\partial t} = \nabla \times (\bar{\mathbf{U}} \times \bar{\mathbf{B}} + \bar{\mathcal{E}} - \eta \mu_0 \bar{\mathbf{J}}), \quad (1)$$

$$\frac{D\alpha_M}{Dt} = -2\eta_t k_f^2 \left(\frac{\bar{\mathcal{E}} \cdot \bar{\mathbf{B}}}{B_{\text{eq}}^2} + \frac{\alpha_M}{R_m} \right), \quad (2)$$

where $\bar{\mathbf{B}}$ is the mean magnetic field, $\bar{\mathbf{J}} = \nabla \times \bar{\mathbf{B}}/\mu_0$ is the mean current density, μ_0 is the vacuum permeability, η is the microscopic magnetic Spitzer diffusivity, η_t is the turbulent magnetic diffusivity,

$$R_m = \eta_t/\eta \quad (3)$$

is here used as the definition of the magnetic Reynolds number, k_f is the wavenumber of the energy-carrying

scale, $D/Dt = \partial/\partial t + \bar{\mathbf{U}} \cdot \nabla$ is the advective derivative with respect to the mean flow $\bar{\mathbf{U}}$, and

$$\bar{\mathcal{E}} = q(\alpha \bar{\mathbf{B}} - \eta_t \mu_0 \bar{\mathbf{J}}) \quad (4)$$

is the turbulent electromotive force (assuming local isotropy), with an *ad hoc* added overall quenching of the electromotive force via the factor

$$q = 1/(1 + q_B \bar{\mathbf{B}}^2/B_{\text{eq}}^2). \quad (5)$$

Such an overall quenching was applied also in the recent dynamically quenched mean field of Brandenburg & Subramanian (2005b).

Under the assumption of locally isotropic turbulence we have $\alpha = \alpha_K + \alpha_M$, where $\alpha_K = -\frac{1}{3}\tau \overline{\boldsymbol{\omega} \cdot \mathbf{u}}$ is the kinetic α effect, where $\boldsymbol{\omega} = \nabla \times \mathbf{u}$ is the vorticity, $\alpha_M = \frac{1}{3}\tau \overline{\mathbf{j} \cdot \mathbf{b}}/\rho_0$ is the magnetic contribution to the α effect, and $\eta_t = \frac{1}{3}\tau \overline{\mathbf{u}^2}$ is turbulent magnetic diffusivity. In deriving equation (2) we have used the definitions $B_{\text{eq}}^2 = \mu_0 \rho u^2$ and $\eta_t = \frac{1}{3}\tau u^2$, so that $\frac{1}{3}\tau/(\mu_0 \rho) = B_{\text{eq}}^2/\eta_t$ (see Blackman & Brandenburg 2002).

Equation (2) can now be solved together with equation (1) to determine the effect of magnetic helicity evolution on the solar dynamo. These equations have been solved in recent years both in context of the galactic dynamo (Kleeorin et al. 2000, 2002, Shukurov et al. 2005) and the solar dynamo (Kleeorin et al. 2003, Zhang et al. 2006). The dynamical quenching model has also been tested against direct simulations (Blackman & Brandenburg 2002, Brandenburg & Subramanian 2005b).

We emphasize however that, although $\bar{\mathbf{B}}$ depends only on x and y , $\bar{\mathbf{U}}$ depends also on z in a prescribed fashion, such as to model the radial differential rotation. To ensure that the field stays numerically divergence free, it is advantageous to write equation (1) in terms of the mean magnetic vector potential $\bar{\mathbf{A}}$, so $\bar{\mathbf{B}} = \nabla \times \bar{\mathbf{A}}$ and the radial velocity gradient is explicitly added to the model by working with the velocity in the form

$$\bar{\mathbf{U}} = \bar{\mathbf{U}}^{(0)}(z) + \bar{\mathbf{u}}(x, y, t); \quad \bar{\mathbf{U}}^{(0)} = (Sz, 0, 0). \quad (6)$$

We apply the equations at the reference height $z = 0$, so $\bar{\mathbf{U}}^{(0)}$ itself is zero and does not enter the equations; only a single component of its derivative matrix, $\bar{U}_{x,z}^{(0)} = S$, enters. Thus, the full set of equations is

$$\frac{D\bar{A}_i}{Dt} = -\bar{U}_{j,i}\bar{A}_j + \bar{\mathcal{E}}_i + \eta \nabla^2 \bar{A}_i, \quad (7)$$

$$\frac{D\bar{U}_i}{Dt} = -\bar{U}_{i,j}\bar{U}_j - c_s^2 \nabla_i \ln \rho + \rho^{-1}(\bar{\mathbf{J}} \times \bar{\mathbf{B}})_i, \quad (8)$$

$$\frac{D \ln \rho}{Dt} = -\nabla \cdot \bar{\mathbf{U}}, \quad (9)$$

$$\frac{D\alpha_M}{Dt} = -2\eta_t k_f^2 \left(\frac{\bar{\mathcal{E}} \cdot \bar{\mathbf{B}}}{B_{\text{eq}}^2} + \frac{\alpha_M}{R_m} \right). \quad (10)$$

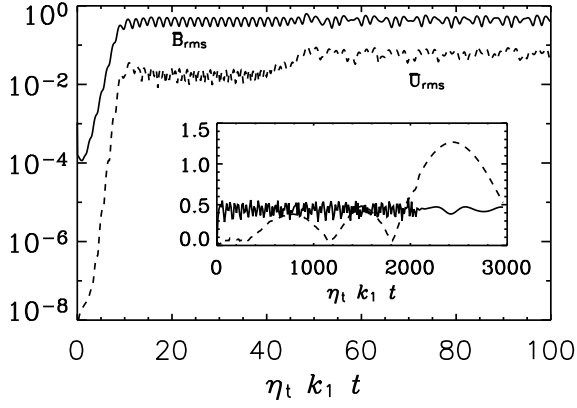


Figure 1. Time dependence of the rms mean magnetic field and the rms mean velocity, showing the emergence of oscillatory and later more irregular solutions.

We model the magnetic field only in one hemisphere and restrict ourselves to dipolar parity by demanding

$$\overline{A}_{x,y} = \overline{A}_y = \overline{A}_{z,y} = 0 \quad (\text{on } y = 0), \quad (11)$$

corresponding to a normal-field condition ($\hat{n} \times \overline{\mathbf{B}} = 0$), modeling the equator, and

$$\overline{A}_x = \overline{A}_{y,y} = \overline{A}_z = 0 \quad (\text{on } y = 2\pi), \quad (12)$$

corresponding to a perfect conductor boundary condition ($\hat{n} \cdot \overline{\mathbf{B}} = 0$), in an attempt to capture some of the behavior on the pole. The simulations have been carried out using the PENCIL CODE¹ which is a high-order finite-difference code (sixth order in space and third order in time) for solving the compressible hydromagnetic equations. The code comes with a special mean field module for the dynamical α quenching equations.

3. RESULTS

In the following we discuss in detail one particular model using the following set of parameters: $S = -30$ (corresponding to negative radial differential rotation), $\alpha_K = 0.5$, $\nu_t = \eta_t = 1$, $\eta = 0.05$ (so $R_m = 20$), $k_f = 5$, and an overall quenching factor with $q_B = 0.1$.

In Fig. 1 we show the evolution of the rms values of the mean magnetic field, $\langle \overline{\mathbf{B}}^2 \rangle^{1/2}$ and of the mean velocity field, $\langle \overline{\mathbf{U}}^2 \rangle^{1/2}$. Initially, the magnetic field grows exponentially, but then it saturates in an oscillatory fashion. The mean field also drives a mean flow. The long time behavior is more complicated, as is shown in the inset: the velocity increases slightly, but then the field becomes

¹<http://www.nordita.dk/software/pencil-code>

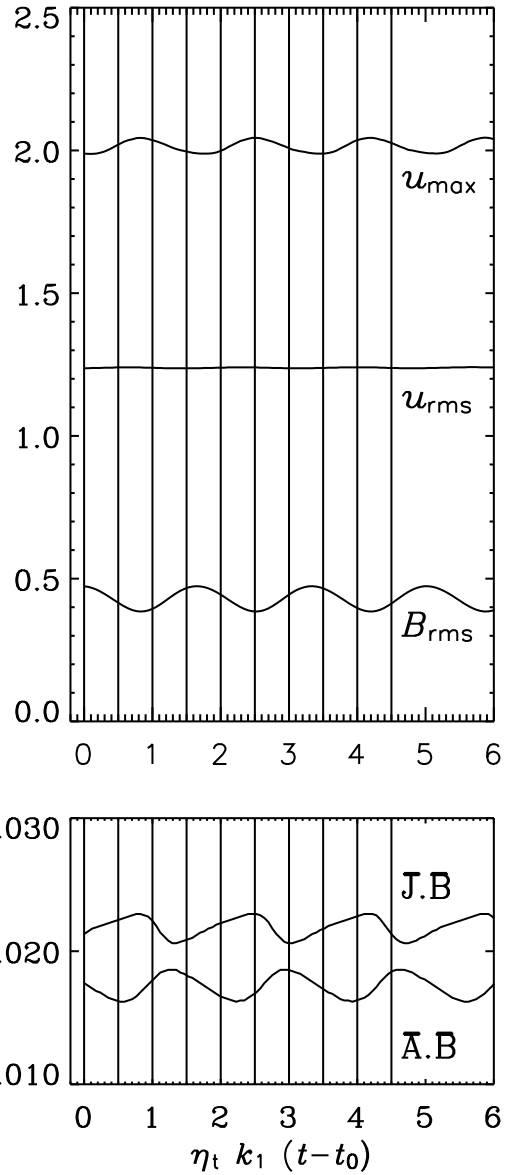


Figure 2. Time dependence of various integral quantities, in the quiescent phase after $\eta_t k_1 t_0 = 2700$. The vertical bars indicate the times for which synthetic ‘magnetograms’ and plots of other quantities are given below.

more irregular. There are also stages where the velocity exceeds the magnetic field and limits the time dependence.

In Fig. 2 we show the evolution of the rms values of velocity and magnetic field, as well as the maximum velocity, together with the mean magnetic and current helicities, $\langle \overline{\mathbf{A}} \cdot \overline{\mathbf{B}} \rangle$ and $\langle \overline{\mathbf{J}} \cdot \overline{\mathbf{B}} \rangle$ during a short time interval during a quiescent stage. The vertical bars mark the times for which snapshots of various quantities are shown in Figs 3–5 that will be discussed next.

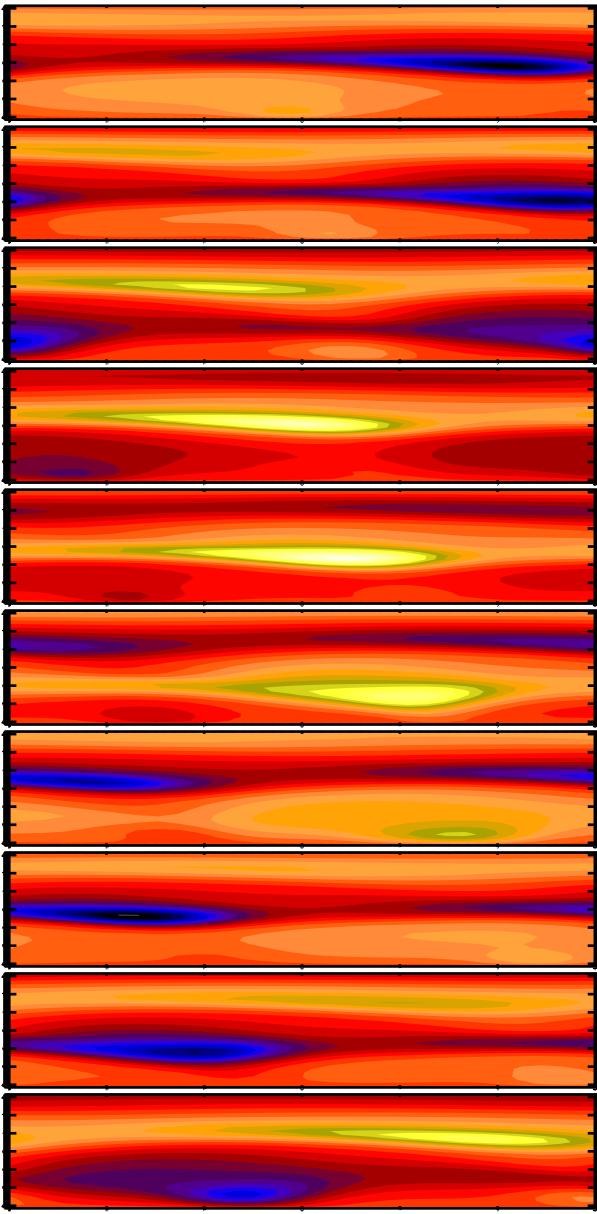


Figure 3. Plot of $\overline{B}_z(x, y)$ at different times, in regular intervals of $\eta_t k_1 \Delta t = 0.5$ after $t = t_0$.

We begin with Fig. 3, where we show images of the line of sight component of the magnetic field, \overline{B}_z . One clearly sees magnetic activity patches moving both equatorward (downward in the plot) as well as in the prograde direction (to the right in the plot). The fact that these patches propagate at all is interesting. It is not related to a locally enhanced mean flow in the prograde direction: the flow is actually in the retrograde direction. The propagation must therefore be related to a proper three-dimensional dynamo mode travelling to the right, just like in the non-axisymmetric dynamo models mentioned in the beginning.

Next, we consider images of current helicity, $\overline{\mathbf{J}} \cdot \overline{\mathbf{B}}$, in

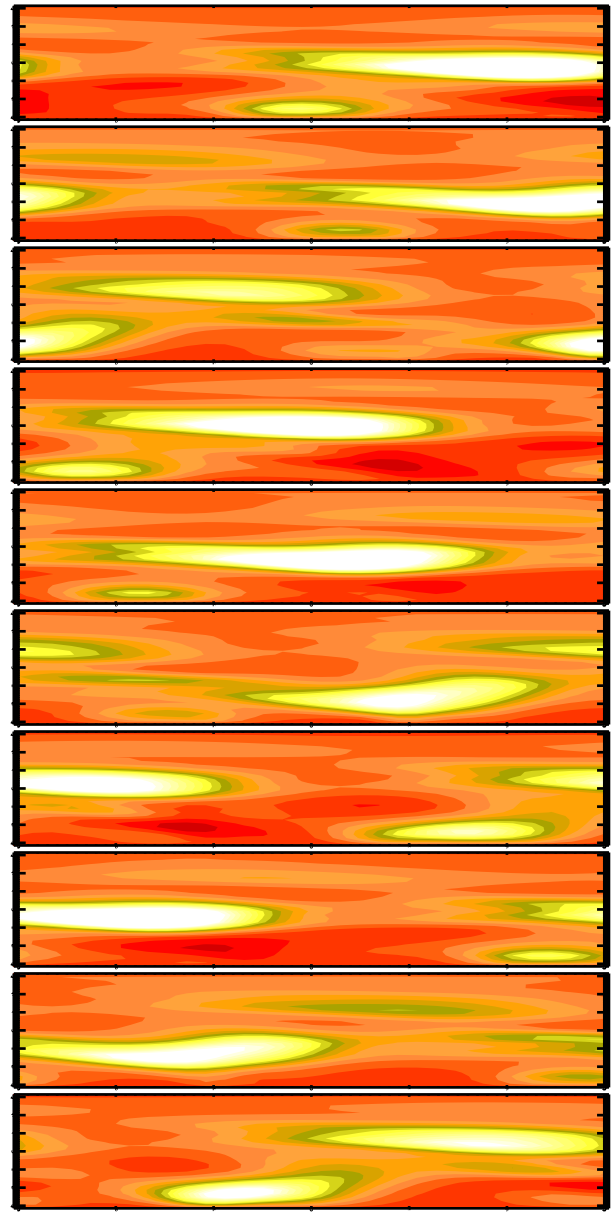


Figure 4. Plot of $\overline{\mathbf{J}} \cdot \overline{\mathbf{B}}$ at different times, in regular intervals of $\eta_t k_1 \Delta t = 0.5$ after $t = t_0$.

Fig. 4, which clearly shows enhanced positive current helicity in the regions where also the line-of-sight magnetic field is strong. The current helicity has the same sign in the magnetic patches with positive and negative net flux.

Finally, we consider images of the magnetic α effect. The connection between α_M and field strength or current helicity is not very clear. Indeed, the two are only loosely connected with each other. The primary reason for having the magnetic α term is to provide a nonlinear feedback between the produced large scale helicity and the α effect that helps to maintain total magnetic helicity conservation.

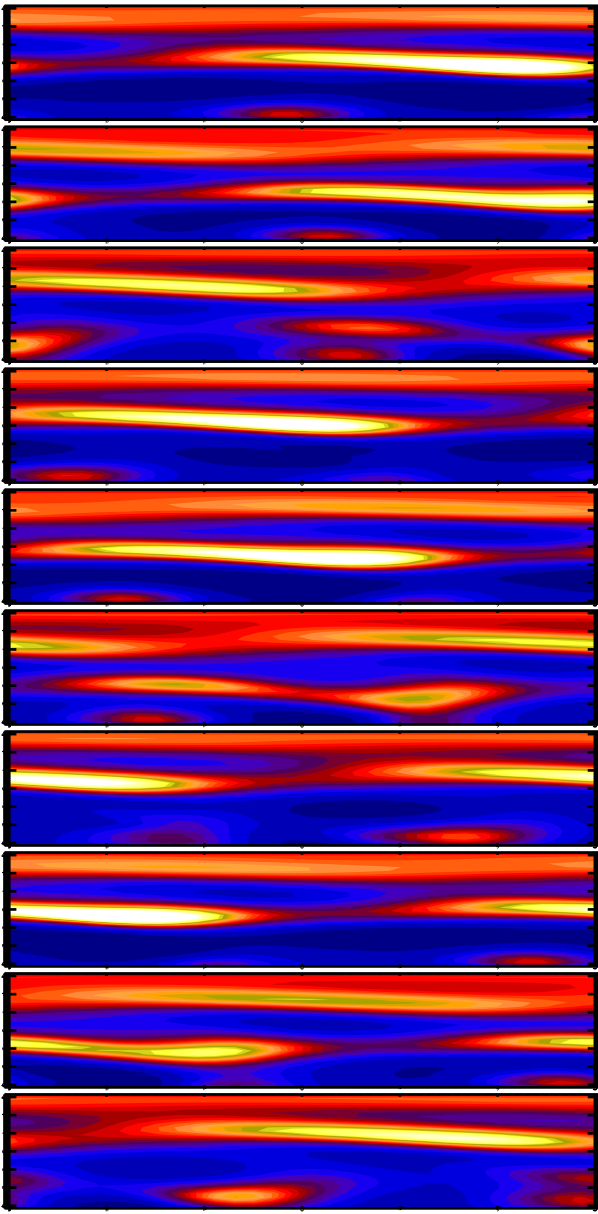


Figure 5. Plot of $\alpha_M(x, y)$ at different times, in regular intervals of $\eta_t k_1 \Delta t = 0.5$ after $t = t_0$.

4. CONCLUSIONS

The present investigations can only be regarded as preliminary, because we have not been able to explore the big parameter space given by the large number of unknowns. Most worrisome is the restriction to only small values of the magnetic Reynolds number. At the moment we are experiencing problems when we try larger values, suggesting that the problem may not be well-posed for larger values of R_m and may require modifications. However, this is still surprising, because similar problems have not been encountered in simpler problems, where however no mean advection or shear was taken into ac-

count (e.g. Brandenburg & Subramanian 2005b).

One surprising aspect emerging from the present simulations is the fact that magnetic patterns do not move with the local gas velocity. Instead, the field propagation is governed by the nonaxisymmetric dynamics of the dynamo modes. Thus, these simulations would not support the notion of field line anchoring. This picture is occasionally used in connection with sunspot proper motions. Long before the internal angular velocity was determined via helioseismology, it was known that sunspots rotate faster than the surface plasma (Howard et al. 1984). Moreover, young sunspots rotate faster than old sunspots (Tuominen & Virtanen 1988, Pulkkinen & Tuominen 1998). A common interpretation is that young sunspots are still anchored at a greater depth than older ones, and that therefore the internal angular velocity must increase with depth (see also Brandenburg 2005). This provided also the basis for the classical mean field dynamo theory of the solar cycle according to which the radial angular velocity gradient has to be negative (Parker 1987).

Given the lack of agreement between the speed of magnetic patches and the local flow speed, one it led to believe that magnetic structures can therefore not be used as tracers of the local flow speed. Alternatively, it is also possible that the tracer properties of the advected field are fully displayed only in three dimensions, or at larger magnetic Reynolds numbers. However, the present results should be interpreted with care, because the present calculations have only been possible in a rather limited parameter range and for rather small magnetic Reynolds numbers. It would be important to test the notion of field line anchoring in direct simulations of the original non-averaged equations, i.e. in the presence of developed turbulence.

ACKNOWLEDGMENTS

The Danish Center for Scientific Computing is acknowledged for granting time on the Horseshoe cluster.

REFERENCES

- Bai, T. 1987, ApJ, 314, 795
- Bai, T. 1988, ApJ, 328, 860
- Bai, T. 2003, ApJ, 585, 1114
- Benevolenskaya, E. E., Hoeksema, J. T., Kosovichev, A. G., & Scherrer, P. H. 1999, ApJ, 517, L163
- Berdugina, S. V., & Usoskin, I. G. 2003, A&A, 405, 1121
- Berdugina, S. V., Moss, D., Sokoloff, D., & Usoskin, I. G. 2006, A&A, 445, 703
- Bigazzi, A., & Ruzmaikin, A. 2004, ApJ, 604, 944
- Blackman, E. G., & Brandenburg, A. 2002, ApJ, 579, 359
- Bogart, R. S. 1982, Solar Phys., 76, 155

Brandenburg, A. 2001, ApJ, 550, 824
Brandenburg, A. 2005, ApJ, 625, 539
Brandenburg, A., & Subramanian, K. 2005a, Phys. Rep., 417, 1
Brandenburg, A., & Subramanian, K. 2005b, AN, 326, 400
Field, G. B., & Blackman, E. G. 2002, ApJ, 572, 685
Ji, H. 1999, PRL, 83, 3198
Kleeorin, N., Moss, D., Rogachevskii, I., & Sokoloff, D. 2000, A&A, 361, L5
Kleeorin, N., Moss, D., Rogachevskii, I., & Sokoloff, D. 2002, A&A, 387, 453
Kleeorin, N., Kuzanyan, K., Moss, D., Rogachevskii, I., Sokoloff, D., & Zhang, H. 2003, A&A, 409, 1097
Moss D. 1999, MNRAS, 306, 300
Moss D. 2004, MNRAS, 352, L17
Moss, D., & Brooke, J. 2000, MNRAS, 315, 735
Moss, D., Barker, D. M., Brandenburg, A., & Tuominen, I. 1995, A&A, 294, 155
Pelt, J., Tuominen, I., & Brooke, J. 2005, A&A, 429, 1093
Pouquet, A., Frisch, U., & Léorat, J. 1976, JFM, 77, 321
Rädler, K.-H., Wiedemann, E., Brandenburg, A., Meinel, R., & Tuominen, I. 1990, A&A, 239, 413
Shukurov, A., Sokoloff, D., Subramanian, K., & Brandenburg, A. 2005, A&A, (submitted, arXiv: astro-ph/0512592)
Subramanian, K. 2002, Bull. Astr. Soc. India, 30, 715
Usoskin, I. G., Berdyugina, S. V., & Poutanen, J. 2005, A&A, 441, 347
Vitinskij, J. I. 1969, Solar Phys., 7, 210
Zhang, H., Sokoloff, D., Rogachevskii, I., Moss, D., Lamburt, V., Kuzanyan, K., & Kleeorin, N. 2006, MNRAS, 365, 276